



HAL
open science

Asymmetrical response of dayside ion precipitation to a large rotation of the IMF

J. Berchem, R. L. Richard, C. P. Escoubet, S. Wing, F. Pitout

► **To cite this version:**

J. Berchem, R. L. Richard, C. P. Escoubet, S. Wing, F. Pitout. Asymmetrical response of dayside ion precipitation to a large rotation of the IMF. *Journal of Geophysical Research Space Physics*, 2016, 121, pp.263-273. 10.1002/2015JA021969 . insu-03670555

HAL Id: insu-03670555

<https://insu.hal.science/insu-03670555>

Submitted on 17 May 2022

HAL is a multi-disciplinary open access archive for the deposit and dissemination of scientific research documents, whether they are published or not. The documents may come from teaching and research institutions in France or abroad, or from public or private research centers.

L'archive ouverte pluridisciplinaire **HAL**, est destinée au dépôt et à la diffusion de documents scientifiques de niveau recherche, publiés ou non, émanant des établissements d'enseignement et de recherche français ou étrangers, des laboratoires publics ou privés.

Copyright

RESEARCH ARTICLE

10.1002/2015JA021969

Key Points:

- Dayside ion precipitation develops a north-south asymmetry in response to a large IMF rotation
- A spot of high-energy particle injections is found in one hemisphere but not in the other
- The asymmetry results from the draping of newly opened field lines over the dayside magnetosphere

Correspondence to:

J. Berchem,
jberchem@ucla.edu

Citation:

Berchem, J., R. L. Richard, C. P. Escoubet, S. Wing, and F. Pitout (2016), Asymmetrical response of dayside ion precipitation to a large rotation of the IMF, *J. Geophys. Res. Space Physics*, 121, 263–273, doi:10.1002/2015JA021969.

Received 1 OCT 2015

Accepted 12 DEC 2015

Accepted article online 16 DEC 2015

Published online 19 JAN 2016

Asymmetrical response of dayside ion precipitation to a large rotation of the IMF

J. Berchem¹, R. L. Richard¹, C. P. Escoubet², S. Wing³, and F. Pitout^{4,5}

¹Department of Physics and Astronomy, University of California, Los Angeles, California, USA, ²ESA, ESTEC, Noordwijk, Netherlands, ³The Johns Hopkins University Applied Physics Laboratory, Laurel, Maryland, USA, ⁴University of Toulouse, UPS-OMP, IRAP, Toulouse, France, ⁵CNRS, IRAP, Toulouse, France

Abstract We have carried out global magnetohydrodynamics (MHD) simulations together with large-scale kinetic simulations to investigate the response of the dayside magnetospheric ion precipitation to a large rotation (135°) of the interplanetary magnetic field (IMF). The study uses simplified global MHD model (no dipole tilt and constant ionospheric conductance) and idealized solar wind conditions where the IMF rotates smoothly from a southward toward a northward direction ($B_x = 0$) to clearly identify the effects of the impact of the discontinuity on the magnetopause. Results of the global simulations reveal that a strong north-south asymmetry develops in the pattern of precipitating ions during the interaction of the IMF rotation with the magnetopause. For a counterclockwise IMF rotation from its original southward direction ($B_y < 0$), a spot of high-energy particle injections occurs in the Northern Hemisphere but not in the Southern Hemisphere. The spot moves poleward and dawnward as the interacting field rotates. In that case, reconnection is found close to the poleward edge of the northern cusp, while it occurs farther tailward in the Southern Hemisphere. Tracing magnetic field lines shows an asymmetry in the tilt of the cusps and indicates that the draping and subsequent double reconnection of newly opened field lines from the Southern Hemisphere over the dayside magnetosphere cause the symmetry breaking. The reverse north-south asymmetry is found for a clockwise IMF rotation from its original southward direction ($B_y > 0$). Trends observed in the ion dispersions predicted from the simulations are in good agreement with Cluster observations of the midaltitude northern cusp, which motivated the study.

1. Introduction

A large number of the asymmetries identified in the magnetosheath, magnetosphere, and ionosphere have been connected to the direction of the B_y component of the interplanetary magnetic field (IMF). For example, it has been shown that the presence of a significant IMF B_y component creates dawn-dusk asymmetries in magnetosheath densities near solar maximum [Paularena et al., 2001], plasma convection [Heppner, 1972; Svalgaard, 1973; Volland, 1975; Mozer et al., 1974; Cowley and Lockwood, 1992; Weimer, 1995; Grocott and Milan, 2014], densities in the distant tail lobes [Gosling et al., 1985], source regions of field-aligned currents and particle precipitation [Wing et al., 2010], and poleward moving auroral forms [Sandholt and Farrugia, 2007]. Hence, it is not surprising that the first studies of particle precipitating in the cusps reported some IMF B_y driven dawn-dusk asymmetries in particle precipitation [e.g., Burch et al., 1985; Newell et al., 1989] though a few investigations noticed a systematic asymmetry of the cusp precipitation, which was independent of the IMF direction [e.g., Meng, 1981; Zhao et al., 1999; Stubbs et al., 2001]. Studies have also shown that the IMF B_y component can induce hemispheric asymmetries. For example, a north-south asymmetry has been observed in the ionospheric response to tail reconnection during IMF northward nonsubstorm intervals [Grocott et al., 2005]. More recently, Förster and Haaland [2015] used observations from the Cluster Electron Drift Instrument to show that the rotation of the main two-cell convection pattern is determined by the sign of IMF B_y and that the phase change of that rotation has an opposite orientation in the opposite hemispheres.

Past studies using global MHD simulations in conjunction with large-scale kinetic (LSK) calculations to determine the entry of solar wind ions in the magnetosphere confirmed that the B_y component and history of the IMF, as well as nonadiabatic acceleration of ions at the magnetopause, could cause significant asymmetries [Richard et al., 1994; Peromian, 2003]. However, more recent MHD-LSK simulations revealed that an unexpected dawn-dusk asymmetry in the precipitation of low- to middle-energy ions develops during periods of steady southward IMF [Berchem et al., 2014]. The study showed that the resistive part of the

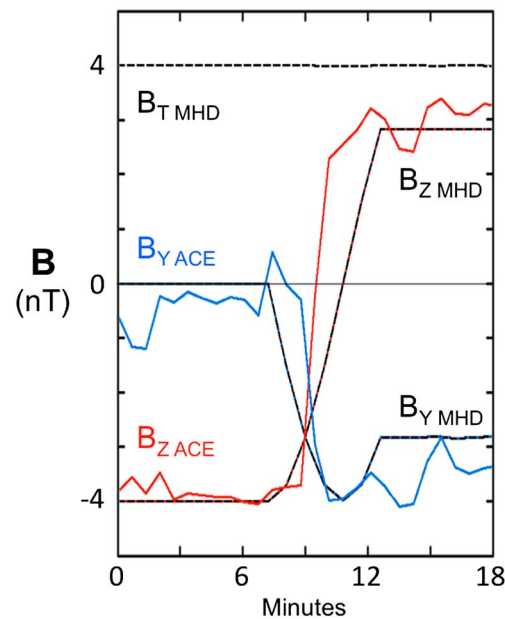


Figure 1. The blue and red traces display the B_Y and B_Z components, respectively, of the IMF rotation observed by ACE around 14:20 UT on 23 September 2004, which was used to determine the idealized magnetic field input used in the MHD simulations (black lines).

magnetopause's parallel electric field ($E_{\parallel} = \eta j_{\parallel}$) points toward the ionosphere in the prenoon sector and outward in the afternoon sector. Hence, the dawn-dusk asymmetry found in the ion precipitation predicted by the LSK simulation results from the reversal of the parallel electric field across the noon-midnight meridian. Although the directions of the parallel electric fields at dawn and dusk in the Southern Hemisphere are opposite to those in the Northern Hemisphere, no interhemispheric asymmetry occurs. The same dawn-dusk asymmetry, parallel electric field inward on the dawnside and outward on the duskside, is found in the Southern Hemisphere because the direction of the magnetic field is also opposite with the magnetic field pointing away from Earth in that hemisphere. The asymmetry found in the simulation is consistent with *Wing et al.* [2010] statistical study of more than 20 years of dayside DMSP magnetometer and particle precipitation data, which established that there is more ion precipitation in the open field line regions at dawn-noon sector than at noon-dusk sector.

In this paper we investigate how rotational discontinuities affect the entry of ions at the magnetopause. While the study is motivated by an actual event observed by Cluster [*Escoubet et al.*, 2008], our goal is

not to carry out a detailed comparison with Cluster observations using actual solar wind measurements as input to the simulations [e.g., *Berchem et al.*, 2008]. Here we use a set of idealized solar wind input with a simplified setup of the MHD-LSK simulation model to study how a large IMF rotation affects dayside ion precipitation after a period of steady southward IMF. This methodology allows us to identify clearly the relationships between causes and effects. We find that in addition to the initial dawn-dusk asymmetry formed prior to the impact of the discontinuity, a north-south asymmetry in ion precipitation develops in response to the large rotation of the IMF. We show that this new asymmetry results from the draping of newly reconnected magnetic field lines over the magnetopause, shielding one of the cusps from interacting with incoming solar wind plasma.

2. Modeling Technique

The first step of the studies was to perform a global magnetohydrodynamics (MHD) simulation of the interaction between a large rotation of the IMF with a quasi-steady configuration of the magnetosphere resulting from a period of constant solar wind conditions and southward IMF. We used the global UCLA-MHD code that solves the one-fluid MHD equations [e.g., *Berchem et al.*, 1995; *Raeder et al.*, 1995]. For the study reported here we employed a simulation system that extends $60 R_E$ in the Y and Z directions and $200 R_E$ in the X direction. The grid used was rectangular but nonuniform, with a resolution of about $0.08 R_E$ in the subsolar region and about $0.1 R_E$ in the region where the magnetopause crosses the terminator. Other sources of asymmetry in the simulation model were eliminated by using a uniform Pedersen conductance ($\sigma_p = 5S$), no Hall conductance ($\sigma_H = 0$), and neglecting the tilt of the Earth's magnetic field dipole.

The idealized solar wind input to the MHD simulation was based on an event observed by the Cluster spacecraft when they crossed the northern cusp on 23 September 2004 [*Escoubet et al.*, 2008]. Prior to the event, the IMF B_Z component reversed from south (≈ -4 nT) to north (≈ 3 nT) while the B_Y component went from about 0 nT to -4 nT, such that the IMF made an approximately 130° counterclockwise rotation from its original southward direction. Solar wind velocity and density were quite steady, about 440 km/s and 4 cm^{-3} before the rotation of the magnetic field and about 460 km/s and 4.3 cm^{-3} after it, respectively. Accordingly, the solar wind dynamic pressure increased slightly from about 1.3 nPa to 1.6 nPa.

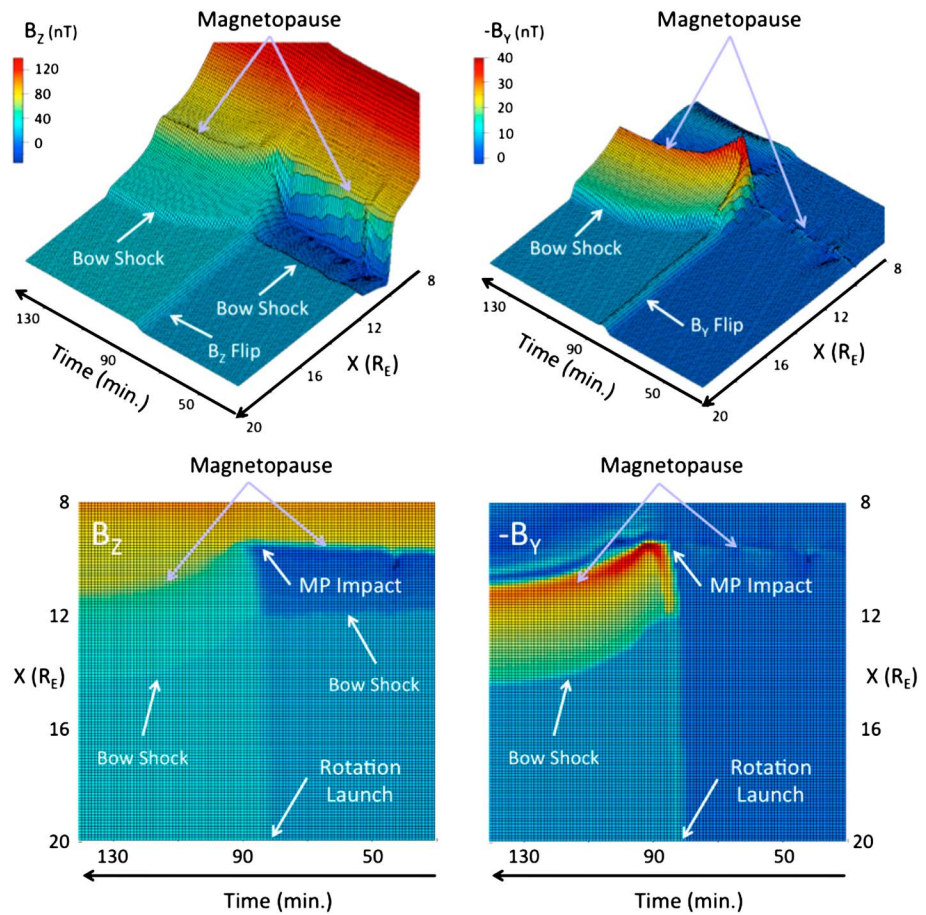


Figure 2. (top row) Perspective views and (bottom row) views from above of the time history of the magnitudes of the (left column) Z and (right column) Y components of the magnetic field along the Sun-Earth line (from $8 R_E$ to $20 R_E$) showing the propagation of the discontinuity through the magnetosheath. The magnitudes of the B_y and B_z components of the magnetic field have been color coded using the scales displayed on the upper left of each column.

To simplify the solar wind plasma conditions for input to the simulation, we used a constant density $n = 4 \text{ cm}^{-3}$ and a constant velocity $V_x = -450 \text{ km/s}$ with $V_y = V_z = 0$. As shown in Figure 1, we also simplified the IMF rotation observed by ACE by smoothing out the field variations, neglecting the B_x component ($B_x = 0$), and keeping the magnitude of the field constant ($B_T = 4 \text{ nT}$) during the entire interval, so $|B_y| = |B_z| = 2.83 \text{ nT}$ at the end of the solar wind rotation. We also moderately increased the duration of the counterclockwise rotation to obtain a clean 5 min 135° rotation.

The next step of the calculation was to perform a large-scale kinetic simulation (LSK) by launching a continuous stream of solar wind particles (about 22×10^6 protons) at the sunward boundary of the MHD simulation system and following their motion in the time-dependent magnetic and electric fields obtained from the MHD simulation [e.g., Richard et al., 1997]. The particles' initial velocities were arranged as drifting Maxwellians centered on the solar wind speed and with a thermal velocity ($v_{th} \approx 22 \text{ km/s}$) corresponding to the solar wind thermal pressure and density employed in the MHD simulation. As a result most of the particles' initial energies were in the $0.980 < E < 1.2 \text{ keV}$ range. Details of the global MHD and LSK modeling technique used to carry out the simulations are described in Berchem et al. [2014].

3. Results

Figure 2 uses the time history of the Z (left column) and Y (right column) components of the magnetic field along the Sun-Earth line to show the propagation of the discontinuity through the magnetosheath. It takes about 4 min for the discontinuity to cross the $3 R_E$ thick magnetosheath, hence an average speed of about

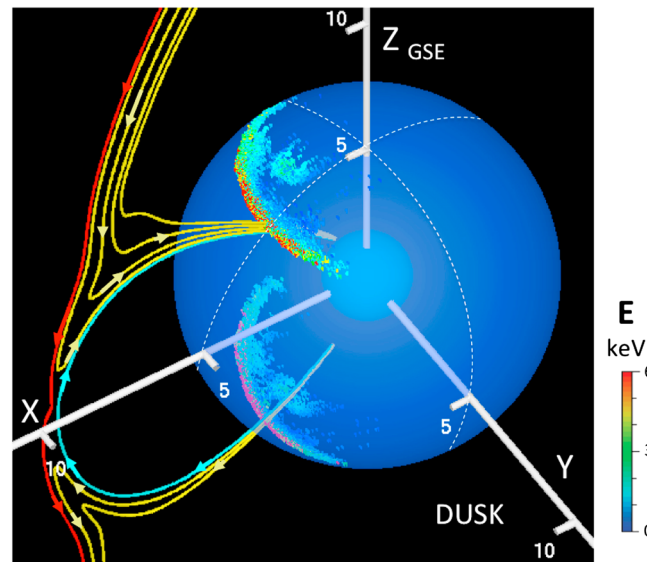


Figure 3. Particle crossings of the spherical detector of radius $5 R_E$ centered on Earth. The translucent blue sphere represents the detector viewed from about 15:00 local time (LT) and about $15 R_E$ above the equatorial plane. The solid blue sphere seen inside the transparent one represents Earth. The white dashed lines indicate the intersection of the spherical detector with the noon-midnight and dawn-dusk meridians. The location of each crossing has been color coded according to the particle's energy using the scale on the right. Only crossings corresponding to earthward motion are displayed. Blue and yellow lines are closed and open field lines, respectively. Red lines show unconnected magnetosheath field lines.

80 km/s, which is of the order of the bulk speed of the flow along the Sun-Earth line in the middle of the magnetosheath and somewhat smaller than the local Alfvén speed.

The impact of the discontinuity on the magnetopause is marked by a clear jump in both field components. The plots also indicate that the magnetosphere starts to expand very quickly after the impact, as shown by the fast sunward motion of the magnetopause and bow shock. As we show below, this sunward motion results from the formation of new magnetospheric flux tubes by double cusp reconnection [e.g., Song and Russell, 1992]. As the IMF rotates toward north, more and more field lines become closed by reconnection between newly reconnected southern field lines draping over the dayside magnetosphere and open field lines from the Northern Hemisphere. It is also interesting to note that the rotation of the 4 nT IMF creates a strong but transient pileup of the magnetic field in front of the subsolar magnetopause. The B_y component, which was 0 before the interaction, reaches a peak of about 40 nT, and it takes about 20 min for the field to settle down to about 24 nT.

Figure 3 shows a spherical detector used in the LSK simulation to collect the locations and velocities of the solar wind particles entering the magnetosphere. It is represented by the transparent blue sphere of radius $5 R_E$ centered on Earth, which is viewed from about 15:00 local time (LT) and $15 R_E$ above the equatorial plane. The location of each ion crossing the detector has been color coded according to the ion's energy at the crossing using the 0–6 keV scale displayed on the right.

All the crossing events displayed in Figure 3 were collected during the period prior to the arrival of the discontinuity when the IMF was purely southward. Magnetic field lines are color coded according to the following scheme that is used throughout this paper. Red lines represent unconnected magnetosheath field lines, while yellow and blue lines indicate open and closed field lines, respectively. The field lines show that reconnection was occurring near the equatorial region, as expected for southward IMF. Looking at the ion crossings, the most energetic ones (red) are observed at low latitudes. These particles are found in the region where the first open field lines intersect the spherical detector, indicating that they were accelerated by the reconnection process [e.g., Reiff et al., 1977]. Middle-energy (yellow) and low-energy (turquoise) particles are observed at progressively higher latitudes. This precipitation pattern is in agreement with the energy-latitude dispersion of particles observed in the cusps, which has been accounted for by the time of flight effect on particles accelerated by reconnection processes occurring in the equatorial region [e.g., Onsager et al., 1993; Wing et al., 1996, 2001].

Figure 3 also reveals a strong dawn-dusk asymmetry in the overall particle precipitation pattern. Since the field lines shown in Figure 3 are traced in the noon-midnight meridian, the locations where they cross the spherical detector can be used to locate local noon. We also display dashed white lines to mark the noon-midnight and dawn-dusk meridians on the detector sphere. Using these guides, it is clear that most of the ion crossings occur in the prenoon and morning sectors; in particular, there is a noticeable patch of

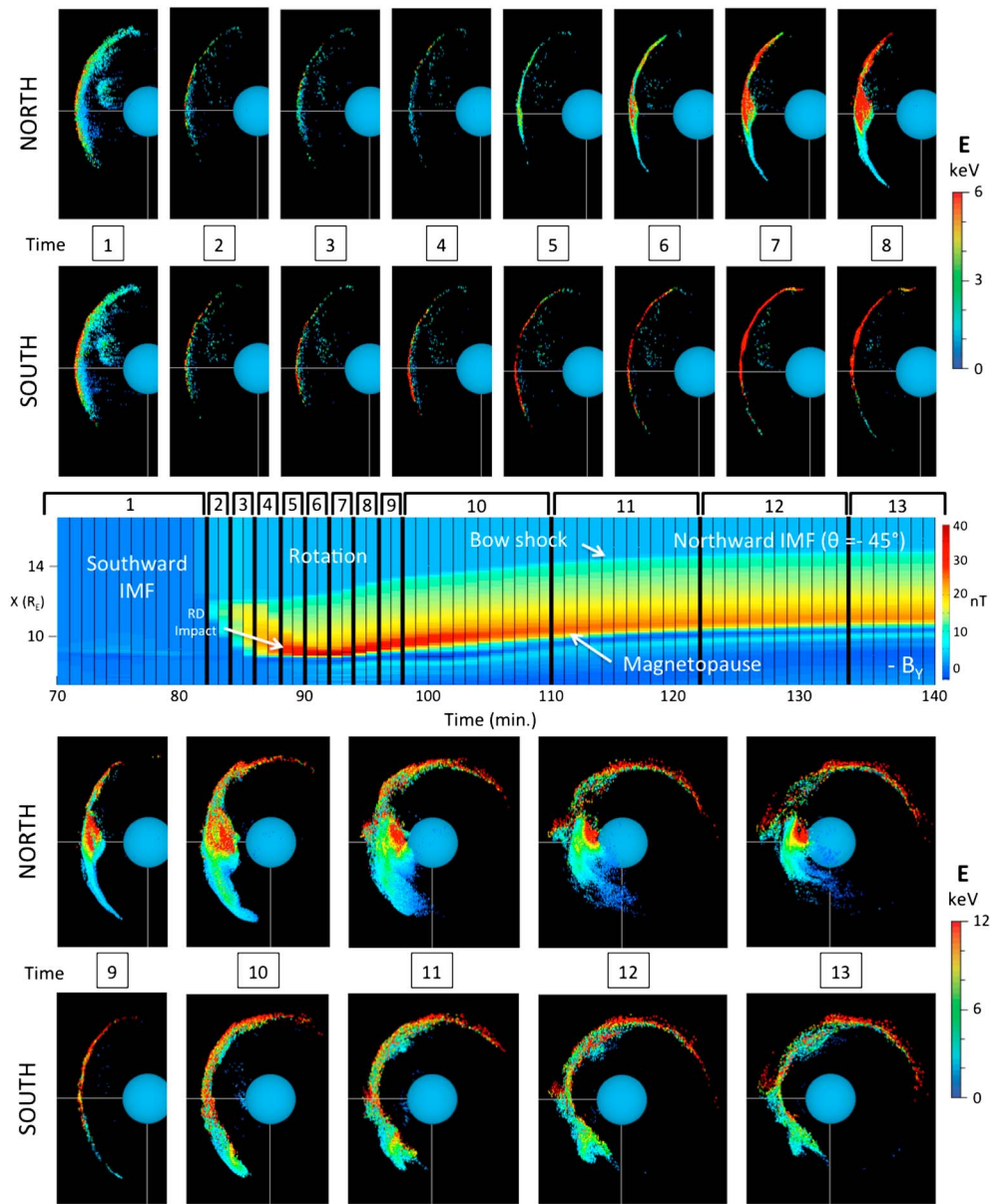


Figure 4. Snapshots of the spherical detector of radius $5 R_E$, which are used to capture the time history of the ion entry throughout the event. (top and bottom) The time series of the northern (top rows) and southern (bottom rows) halves of the detector. Each hemisphere is viewed from above the Northern Hemisphere. Noon is on the left. The location of each particle crossing the detectors has been color coded according to its energy using the scales displayed on the right of Figure 4 (top and bottom). (middle) The time history of the Y component of the magnetic field from the MHD simulation. The magnitude of B_y has been color coded from 0 to 40 nT and is plotted as a function of time measured in minutes from the beginning of the simulation and distance from Earth along the Sun-Earth line within the 8–16 R_E range. The event has been divided into 13 numbered time intervals (TIs) delimited by thick black lines in Figure 4 (middle). Precipitation patterns during each TI are shown in Figure 4 (top and bottom). Snapshots corresponding to TI-1 through TI-8 are shown in Figure 4 (top), while those for TI-9 to TI-13 are shown in Figure 4 (bottom).

precipitating particles at high-latitude prenoon. In contrast, only a narrow band of crossings is visible in the low-latitude afternoon sector. Furthermore, the transparent blue sphere used to represent the spherical detector reveals a similar asymmetry in the Southern Hemisphere. These results are consistent with the previous study [Berchem et al., 2014] that showed that the resistive component of the magnetopause’s parallel electric field ($E_{\parallel} = \eta j_{\parallel}$) has opposite directions in the dawn and dusk regions for purely southward IMF.

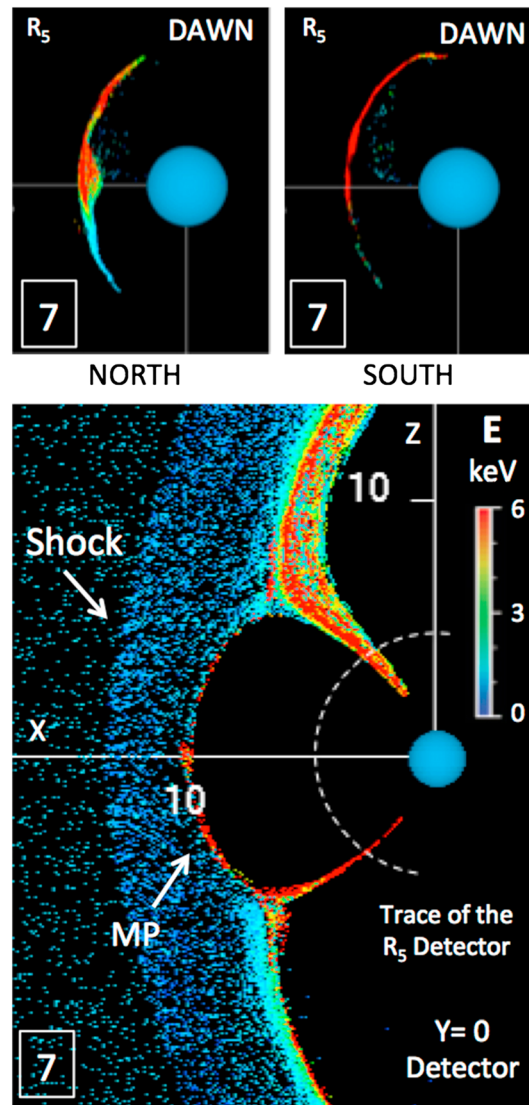


Figure 5. The precipitation patterns in the (top left) north and (top right) south hemispheres, together with a (bottom) snapshot of the planar detector at $Y=0$ viewed from dusk during time interval TI-7. The particle crossings have been color coded according to their energy using the scale displayed on the right of Figure 5 (bottom). The white dashed circle shows the intersection of the planar detector with the spherical detector of radius $5 R_E$.

and southern patterns show the strong dawn-dusk asymmetry mentioned above. Then, a clear asymmetry between the two hemispheres starts to develop when the discontinuity impacts the magnetopause.

At TI-6, high-energy particles form a bulge in the noon sector of the Northern Hemisphere, in contrast to a much narrower range of latitudes in the Southern Hemisphere. Figure 5 relates the precipitation patterns in the north (top left) and south (top right) hemispheres, to a snapshot of the planar detector at $Y=0$ (bottom) viewed from dusk for TI-7. The asymmetric response to the discontinuity observed at TI-5 is now very conspicuous. The planar detector reveals that the northern cusp is populated mostly by energetic ions injected at high latitudes, indicating that the reconnection site has moved from low to high latitude in response to the impact of the discontinuity on the magnetopause. The spread in latitudes seen during the 2 min interval suggests that the reconnection site is moving rapidly to more northern latitudes, explaining the origin of the bulge observed in the Northern Hemisphere. The thin arc of high-energy particles in the southern cusp

Hence, the asymmetry results from the fact that ions reaching the magnetopause on the dawnside are accelerated toward the ionosphere ($E_{\parallel} > 0$), whereas they are accelerated toward the magnetotail on the duskside ($E_{\parallel} < 0$).

Figure 4 illustrates changes in the ion precipitation pattern and their relation to the MHD magnetic field evolution. It consists of three panels, the top and bottom of which have two rows, each showing snapshots of the spherical detector of radius $5 R_E$ (the same as was used for Figure 3) at different times during the event. The time history of the Y component of the magnetic field from the MHD simulation is displayed in Figure 4 (middle), where the magnitude of B_Y has been color coded from 0 to 40 nT. It is plotted as a function of time, measured in minutes from the beginning of the simulation, and distance from Earth along the Sun-Earth line within an $8-16 R_E$ range. The event has been divided into 13 numbered time intervals (TIs) delimited by thick black lines in this panel. Precipitation patterns during each TI are shown in Figure 4 (top and bottom). Snapshots corresponding to TI-1 through TI-8 are shown in Figure 4 (top), while those for TI-9 to TI-13 are shown in Figure 4 (bottom). The top row in each of these panels shows precipitation on the spherical detector in the Northern Hemisphere, and the bottom row shows the Southern Hemisphere. Each hemisphere is viewed from above the Northern Hemisphere. Noon is on the left. The location of each particle crossing the detectors has been color coded according to its energy by using the scales displayed on the right of Figure 4 (top and bottom).

Precipitation patterns in both hemispheres remain similar until TI-5 when the discontinuity impacts the magnetopause. The cusp precipitation from TI-2 to TI-5 appears much thinner than at TI-1 because of the much smaller integration time (2 min versus 15 min) used to produce the snapshots. From the start of the sequence, the northern

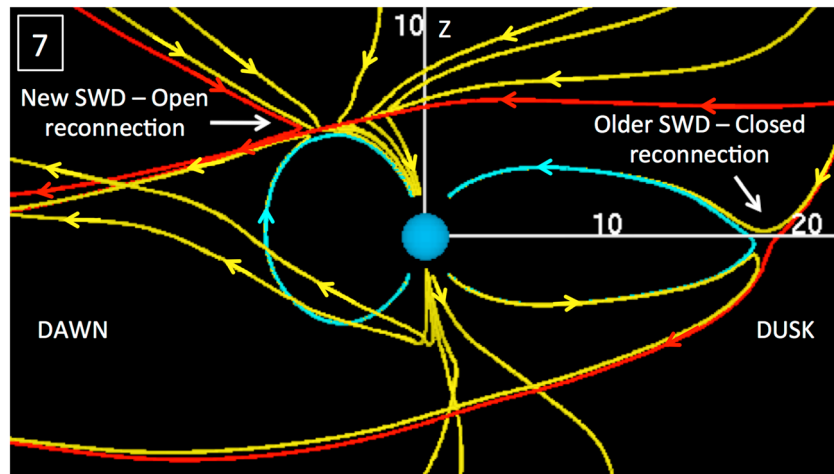


Figure 6. Selected field lines viewed from the Sun for time interval TI-7. Blue and yellow lines are closed and open field lines, respectively. Red lines show unconnected magnetosheath field lines. The wedged unattached red field line seen at dawn in the Northern Hemisphere indicates that at that time, reconnection starts to involve solar wind field lines reconnecting with newly opened field lines. A similar process is not observed in the Southern Hemisphere. On the duskside reconnection remains near the equatorial plane almost unchanged creating a clear dawn-dusk asymmetry in the shape of the magnetosphere.

(Figure 5, top right) and the crossing of high-energy particles recorded by the planar detector at midlatitudes indicate that the reconnection process is also active in the Southern Hemisphere but occurs at lower latitudes than in the Northern Hemisphere.

Figure 6 displays field lines as viewed from the Sun at TI-7. They show that reconnection has started to involve solar wind field lines reconnecting with open field lines (note the wedge-shaped unattached field line on the dawnside in the Northern Hemisphere) forming new closed flux tubes and moving the magnetopause sunward. This process is similar to the one expected to occur poleward of the cusp for purely northward IMF. At this time, convection and draping seem to impede a corresponding process from occurring in the afternoon region of the Southern Hemisphere. Hence, there is a clear dawn-dusk asymmetry in the shape of the magnetosphere: the dawnside is dipolar, while the duskside looks more like a teardrop.

The bulge continues to grow during TI-8 and TI-9, lasting about 4 min (see Figure 4). TI-10 is marked in both hemispheres by a shift of the precipitating particle arcs toward higher latitudes, which appears as a spread in latitude ranges because of the longer integration time used. This development culminates in the formation of a high-energy spot at high latitudes in the Northern Hemisphere at TI-11, a clear signature that reconnection is moving to higher latitudes as the interacting field completes its rotation to a steady northward direction ($\theta = -45^\circ$). A boundary layer of energetic particles (≥ 12 keV) forms from cusp to cusp at the magnetopause. Tracing field lines (not shown here) indicates that the layer results from reconnection occurring in the Southern Hemisphere. Energetic ions are found on both newly closed field lines (double reconnection) and newly reconnected open field lines draping over the magnetopause.

At time TI-12, about 30 min after the discontinuity has impacted the magnetopause, the dayside magnetosphere is approaching a quasi-steady state. The spot of high-energy particles seen in the Northern Hemisphere has reached a stable poleward and dawnward location, indicating that the cusp has moved both in latitude and local time. The initial dawn-dusk asymmetry formed during the period of steady southward IMF prior to the impact of the discontinuity is still present. However, neither a bulge nor a hot spot has formed in the Southern Hemisphere. The absence of these features and the lack of precipitation at high latitudes of the Southern Hemisphere suggest that the IMF with its new orientation ($B_\gamma < 0$) has not interacted with open magnetospheric field lines poleward of the southern cusp. The initial dawn-dusk asymmetry is still present in both hemispheres. Energetic ions are mostly observed in the dawn region where they enter the plasma sheet, while midenergy (≈ 6 keV) ions are now found in the magnetopause boundary layer. Though a patch of high-energy ions remains in the equatorial part of the cusp (on stagnant

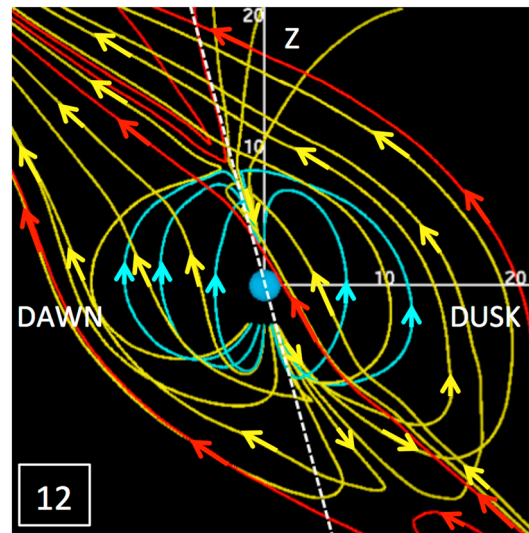


Figure 7. Display of field lines viewed from the Sun for time interval TI-12. Blue and yellow lines are closed and open field lines, respectively. As indicated by the wedge shapes of the newly unconnected field lines (red) reconnection occurs at the poleward edge of the cusp in the Northern Hemisphere, but it is located much farther tailward in the Southern Hemisphere. Open field lines resulting from reconnection in the Southern Hemisphere now drape both the duskside and dawnside of the magnetopause. The dashed line is to emphasize the difference in orientation between the northern and southern cusps.

favors the occurrence of reconnection poleward of the northern cusp, breaking the expected north-south symmetry in the particle precipitation. This process is very similar to the one proposed by *Watanabe et al.* [2007] to explain the interhemispheric potential mismatch of merging cells found in their global MHD simulations for B_y dominated IMF. While in their study reconnection is taking place between draped lobe field lines and closed flank field lines, here reconnection of the draped field lines occurs more poleward because of the more northward orientation of the incoming IMF at the end of its rotation.

Figure 7 also reveals that there is a clear asymmetry in the cusps' locations after the impact of the discontinuity. The dashed line superimposed over the axis of the northern cusp shows that it is tilted about 15° toward dawn, while the southern cusp tilt toward dusk appears larger. Similarly, a dusk view (not shown here) indicates that the sunward tilt of the northern cusp is larger than the southern one. We carried out an additional simulation with similar solar wind conditions but with a clockwise IMF rotation ($B_y > 0$). We found the same patterns but reversed. Ion precipitation occurred at higher latitudes in the Southern Hemisphere than in the Northern Hemisphere. In particular, a high-energy spot formed in the Southern Hemisphere but not in the northern one. It is thus unambiguous that our model predicts that the impact of a large rotation of the IMF on the magnetosphere creates a north-south asymmetry in the global topology of the reconnecting fields at the magnetopause and in the particle precipitation over the dayside magnetosphere.

We are unaware whether north-south asymmetries in dayside ion precipitation have been observed following the impacts of large IMF rotations on the magnetopause. However, *Hu et al.* [2014], in a recent study using observations from all-sky imagers in the Arctic and Antarctica, reported the formation of both a dawn-dusk asymmetry and an interhemispheric asymmetry in electrons precipitating in the dayside auroral oval. They identified two peaks in the auroral emissions at 630.0 nm and 557.7 nm, one in the prenoon sector and the other in the afternoon sector. Comparing their average intensities, they found that the peak observed in the afternoon sector of the Northern Hemisphere was stronger than the peak observed in the prenoon sector and that this dawn-dusk asymmetry reversed in the Southern Hemisphere. *Hu et al.* [2014] suggested that the hemispheric asymmetry resulted from the combined effect of the dawn-dusk variation of the magnetosheath

reconnected southern field lines draping the magnetopause), most of the trapped energetic ions are now drifting around Earth and populating the plasma sheet.

4. Discussion

Tracing field lines for the quasi-steady state reached after the IMF rotation is completed provides additional insight into the origin of the north-south asymmetry found in the precipitation patterns. Figure 7 shows magnetic field lines at TI-12 viewed from the Sun. They reveal a more symmetrical overall magnetospheric shape than at time TI-7 shown in Figure 6. However, a clear asymmetry is still observed in the topology of reconnection. As indicated by the wedge shapes of the newly unconnected field lines (red) appearing at the upper left, reconnection occurs at the poleward edge of the cusp in the Northern Hemisphere. It is located much farther tailward in the Southern Hemisphere. Open field lines resulting from reconnection in the Southern Hemisphere now drape both the duskside and dawnside of the magnetopause. These open field lines shield the southern cusp from interacting with incoming solar wind field lines with the more northward IMF orientation. The resulting topology

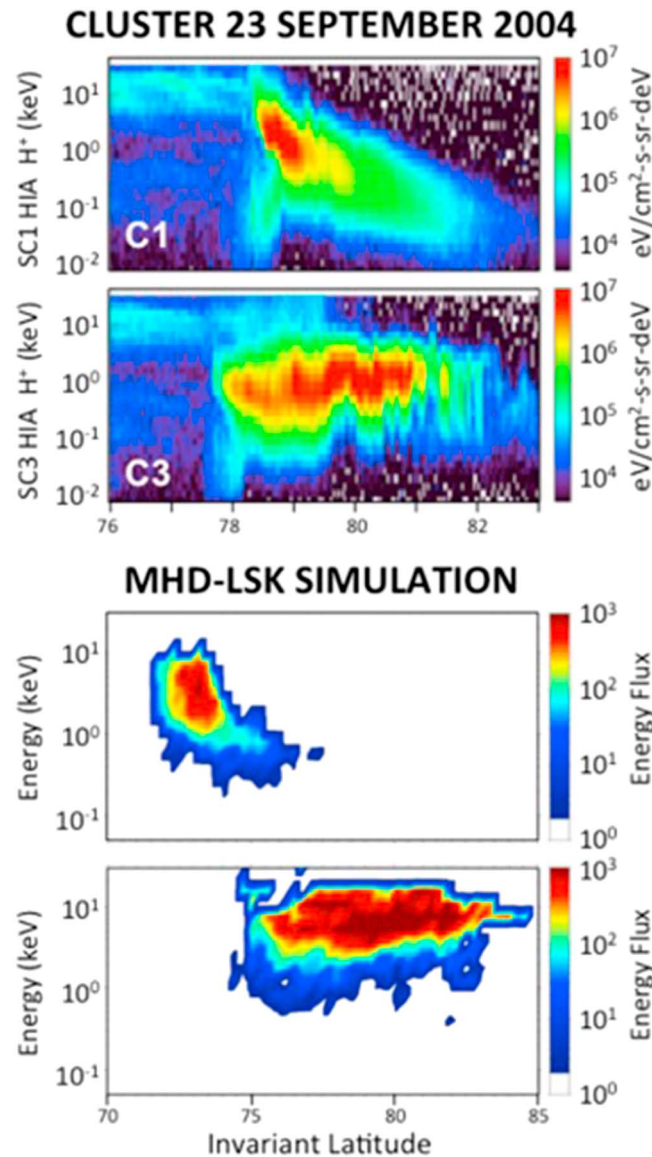


Figure 8. Comparison between energy-latitude dispersions measured by Cluster on 23 September 2004 [Escoubet et al., 2008] and the results of the simulation using an idealized input and simplified model. The calculated dispersions do not include the effects of the relative motion of the spacecraft flying through these structures and assume that their trajectories were lying in the $Y = -1 R_E$ plane. The simulated energy fluxes are displayed using the energy deposited in each latitude-energy bin.

time window (~10 min), so they do not include the effects of the relative motion of the spacecraft flying through these structures. Finally, we used a detector with a high resolution in latitude (0.3°) but large radial bins ($1.0 R_E$) in order to accumulate enough statistics. Because of all these assumptions, and the resulting uncertainties associated with them, we display in Figure 8 energy fluxes using simulation units (i.e., energy deposited in each latitude-energy bin) instead of using particles' initial conditions and detector parameters to rescale them in units that would be directly comparable to those observed by Cluster. This is to emphasize that we are not looking for a quantitative agreement between the simulation results and the observations. The purpose of Figure 8 is to show that despite all these simplifications, the trends observed in the low- and high-energy cutoffs of the ion dispersions obtained from the simulation compare very well with the ones observed

density and the different local ionospheric conductivities at the two observatories. They dismissed any effects of the IMF, in particular, the B_y component. Since they used averaged IMF values over long periods of time, it is unclear how the results of their study relate to our predictions of the ion precipitation following a large rotation of the IMF. While these observations reveal the complex interplay between dawn-dusk and north-south asymmetries, more analyses of simultaneous global observations of ion precipitation in both hemispheres are needed to determine whether inter-hemispheric asymmetries occur after the impact of a large IMF rotation.

Nevertheless, since we modeled the input of our simulations on the solar wind and IMF recorded prior to an event observed by Cluster on 23 September 2004 [Escoubet et al., 2008], we carried out a qualitative comparison of the simulation results with the observations. The result is shown in Figure 8. While we used the same technique as in Berchem et al. [2014] to calculate energy fluxes and produce energy-latitude dispersions from the simulation results, additional assumptions were made. First, as mentioned above, we used a simplified and slower IMF rotation as input together with a simplified simulation model that neglected the significant dipole tilt of Earth at that time ($\approx 11^\circ$ sunward, 25° downward in GSE) and used a constant ionospheric conductance. Second, the ion dispersions shown in Figure 8 were calculated from particle hits collected along the projection of the spacecraft trajectory in the $Y = -1 R_E$ plane, whereas in reality their trajectories were closer to 11:00 magnetic local time meridian. Third, the particle hits were integrated over a long

by Cluster, though there is a shift in the latitude ranges. The energy range found in the simulated dispersion before the impact of the discontinuity is very similar to the ones observed by the Cluster C1 spacecraft. However, the highest energy fluxes calculated after the impact of the discontinuity spread to slightly higher energies than those measured by the Cluster C3 spacecraft. The origin of that discrepancy is unclear. In addition to possible effects related to the assumptions mentioned above, it could be due to the fact that our model does not include wave-particle interactions. Hence, it neglects some energy dissipation processes that could occur in the magnetosheath during the propagation of the discontinuity, as well as during its interaction with the magnetopause. Nevertheless, the overall good qualitative agreement found between the calculated dispersions and the ones observed provides some confidence in the results of the simulation.

5. Summary

We have studied the effects of the interaction of a solar wind rotational discontinuity with the magnetopause. To do so, we carried out global MHD and LSK simulations that used a simplified global MHD model and an idealized input based on the solar wind conditions that were observed prior to the crossing of the midlatitude northern cusp by the Cluster spacecraft on 23 September 2004. During that event the IMF rotated from a southward ($B_Y = 0$) to a northward and dawnward direction ($B_Y < 0$). Using a smooth variation of the IMF clock angle and a simplified magnetospheric geometry of the magnetosphere (no dipole tilt and constant ionospheric conductance) allowed us to clearly identify the effects of the discontinuity as it interacted with the magnetopause. Results of the global simulations revealed that a strong north-south asymmetry in the precipitating particles developed during the interaction of the IMF rotation with the magnetopause. A spot of high-energy injections occurred in the Northern Hemisphere but not in the Southern Hemisphere; the spot moved poleward and dawnward as the interacting field rotated. Reconnection was found close to the poleward edge of the northern cusp, while it occurred farther tailward in the Southern Hemisphere. Tracing magnetic field lines revealed a strong north-south asymmetry in the global topology of the dayside magnetosphere, in particular in the orientation of the cusps. It also indicated that the draping and subsequent double reconnection of newly open field lines from the Southern Hemisphere were at the origin of the symmetry breaking. It was also responsible for the formation of a thick boundary layer of midenergy (≈ 6 keV) ions at the magnetopause. We carried out an additional simulation with similar solar wind conditions but a clockwise IMF rotation ($B_Y > 0$) and found the reverse asymmetry: a spot of high-energy injections was formed in the Southern Hemisphere but not in the Northern Hemisphere. Trends observed in the ion dispersions predicted from the simulations were in good agreement with Cluster observations, though the oversimplified conditions used in the simulations limited the extent of the comparison between the simulation results and the observations.

We are unaware whether north-south asymmetries following the impacts of large IMF rotations on the magnetosphere have been observed but hope that the results of our study will motivate a relevant investigation.

Acknowledgments

The work at UCLA was supported by NASA grant NNX15AI92G, while the support at JHU/APL was provided by NASA grant NNX15AJ01G. This work used computing resources from NASA High-End Computing Program (HEC) and the NSF-supported Extreme Science and Engineering Discovery Environment (XSEDE). Request for simulation data used in this study may be made to J. Berchem.

References

- Berchem, J., J. Raeder, and M. Ashour-Abdalla (1995), Reconnection at the magnetosphere boundary: Results from global magnetohydrodynamics simulations, in *Physics of the Magnetopause*, *Geophys. Monogr. Ser.*, edited by P. Song, B. Sonnerup, and M. Thomsen, pp. 205–213, AGU, Washington, D. C.
- Berchem, J., et al. (2008), Reconnection at the dayside magnetopause: Comparisons of global MHD simulation results with Cluster and Double Star observations, *J. Geophys. Res.*, *113*, A07S12, doi:10.1029/2007JA012743.
- Berchem, J., R. Richard, C. P. Escoubet, S. Wing, and F. Pitout (2014), Dawn-dusk asymmetry in solar wind ion entry and dayside precipitation: Results from large-scale simulations, *J. Geophys. Res. Space Physics*, *119*, 1549–1562, doi:10.1002/2013JA019427.
- Burch, J. L., P. H. Reiff, J. D. Menietti, R. A. Heelis, W. B. Hanson, S. D. Shawhan, E. G. Shelley, M. Sugiura, D. R. Wiemer, and J. D. Winningham (1985), IMF B_Y -dependent plasma flow and Birkeland currents in the dayside magnetosphere: 1. Dynamics Explorer observations, *J. Geophys. Res.*, *90*, 1577–1593, doi:10.1029/JA090iA02p01577.
- Cowley, S. W. H., and M. Lockwood (1992), Excitation and decay of solar wind-driven flows in the magnetosphere-ionosphere system, *Ann. Geophys.*, *10*, 103.
- Escoubet, C. P., et al. (2008), Effect of a northward turning of the interplanetary magnetic field on cusp precipitation as observed by Cluster, *J. Geophys. Res.*, *113*, A07S13, doi:10.1029/2007JA012771.
- Förster, M., and S. Haaland (2015), Interhemispheric differences in ionospheric convection: Cluster EDI observations revisited, *J. Geophys. Res. Space Physics*, *120*, 5805–5823, doi:10.1002/2014JA020774.
- Gosling, J. T., D. N. Baker, S. J. Bame, W. C. Feldman, R. D. Zwickl, and E. J. Smith (1985), North-south and dawn-dusk plasma asymmetries in the distant tail lobes: ISEE 3, *J. Geophys. Res.*, *90*(A7), 6354–6360, doi:10.1029/JA090iA07p06354.
- Grocott, A., and S. E. Milan (2014), The influence of IMF clock angle timescales on the morphology of ionospheric convection, *J. Geophys. Res. Space Physics*, *119*, 5861–5876, doi:10.1002/2014JA020136.

- Grocott, A., T. K. Yeoman, S. E. Milan, and S. W. H. Cowley (2005), Interhemispheric observations of the ionospheric signature of tail reconnection during IMF-northward non-substorm intervals, *Ann. Geophys.*, *23*, 1763–1770.
- Heppner, J. P. (1972), Polar cap electric field distributions related to the interplanetary magnetic field direction, *J. Geophys. Res.*, *77*, 4877–4887, doi:10.1029/JA077i025p04877.
- Hu, Z.-J., Y. Ebihara, H.-G. Yang, H.-Q. Hu, B.-C. Zhang, B. Ni, R. Shi, and T. S. Trondsen (2014), Hemispheric asymmetry of the structure of dayside auroral oval, *Geophys. Res. Lett.*, *41*, 8696–8703, doi:10.1002/2014GL062345.
- Meng, C. I. (1981), Electron precipitation in the midday auroral oval, *J. Geophys. Res.*, *86*, 2149–2174, doi:10.1029/JA086iA04p02149.
- Mozer, F. S., W. D. Gonzalez, F. Bogott, M. C. Kelley, and S. Schutz (1974), High-latitude electric fields and the three-dimensional interaction between the interplanetary and terrestrial magnetic fields, *J. Geophys. Res.*, *79*, 56–63, doi:10.1029/JA079i001p00056.
- Newell, P. T., C.-I. Meng, D. G. Sibeck, and R. Lepping (1989), Some low-latitude cusp dependencies on the interplanetary magnetic field, *J. Geophys. Res.*, *94*, 8921–8927, doi:10.1029/JA094iA07p08921.
- Onsager, T. G., C. A. Kletzing, J. B. Austin, and H. MacKiernan (1993), Model of magnetosheath plasma in the magnetosphere: Cusp and mantle particles at low-latitudes, *Geophys. Res. Lett.*, *20*, 479–482, doi:10.1029/93GL00596.
- Paularena, K. I., J. D. Richardson, M. A. Kolpak, C. R. Jackson, and G. L. Siscoe (2001), A dawn-dusk density asymmetry in Earth's magnetosheath, *J. Geophys. Res.*, *106*(A11), 25,377–25,394, doi:10.1029/2000JA000177.
- Peromian, V. (2003), The influence of the interplanetary magnetic field on the entry of solar wind ions into the magnetosphere, *Geophys. Res. Lett.*, *30*(7), 1407, doi:10.1029/2002GL016627.
- Raedel, J., R. J. Walker, and M. Ashour-Abdalla (1995), The structure of the distant geomagnetic tail during long periods of northward IMF, *Geophys. Res. Lett.*, *22*, 349–352, doi:10.1029/94GL03380.
- Reiff, P. H., T. W. Hill, and J. L. Burch (1977), Solar wind plasma injection at the dayside magnetospheric cusp, *J. Geophys. Res.*, *82*, 479–491, doi:10.1029/JA082i004p00479.
- Richard, R. L., R. J. Walker, and M. Ashour-Abdalla (1994), The population of the magnetosphere by solar wind ions when the interplanetary magnetic field is northward, *Geophys. Res. Lett.*, *21*, 2455–2458.
- Richard, R. L., R. J. Walker, T. Ogino, and M. Ashour-Abdalla (1997), Flux ropes in the magnetotail: Consequences for ion populations, *Adv. Space Res.*, *20*, 1017–1021.
- Sandholt, P. E., and C. J. Farrugia (2007), Role of poleward moving auroral forms in the dawn-dusk auroral precipitation asymmetries induced by IMF B_y , *J. Geophys. Res.*, *112*, A04203, doi:10.1029/2006JA011952.
- Song, P., and C. T. Russell (1992), Model of the formation of the low-latitude boundary layer for strongly northward interplanetary magnetic field, *J. Geophys. Res.*, *97*, 1411–1420, doi:10.1029/91JA02377.
- Stubbs, T. J., M. Lockwood, P. Cargill, J. Fennell, M. Grande, B. Kellett, C. Perry, and A. Rees (2001), A dawn-dusk asymmetry in particles of solar wind origin within the magnetosphere, *Ann. Geophys.*, *19*, 1–9, doi:10.5194/angeo-19-1-2001.
- Svalgaard, L. (1973), Polar cap magnetic variations and their relationship with the interplanetary magnetic sector structure, *J. Geophys. Res.*, *78*, 2064–2078, doi:10.1029/JA078i013p02064.
- Volland, H. (1975), Differential rotation of the magnetospheric plasma as cause of the Svalgaard-Mansurov effect, *J. Geophys. Res.*, *80*, 2311–2315, doi:10.1029/JA080i016p02311.
- Watanabe, M., G. J. Sofko, K. Kabin, R. Rankin, A. J. Ridley, C. R. Clauer, and T. I. Gombosi (2007), Origin of the interhemispheric potential mismatch of merging cells for interplanetary magnetic field B_y -dominated periods, *J. Geophys. Res.*, *112*, A10205, doi:10.1029/2006JA012179.
- Weimer, D. R. (1995), Models of high-latitude electric potentials derived with a least error fit of spherical harmonic coefficients, *J. Geophys. Res.*, *100*, 19,595–19,607, doi:10.1029/95JA01755.
- Wing, S., P. T. Newell, and T. G. Onsager (1996), Modeling the entry of the magnetosheath electrons into the dayside ionosphere, *J. Geophys. Res.*, *101*, 13,155–13,167, doi:10.1029/96JA00395.
- Wing, S., P. T. Newell, and J. M. Ruohoniemi (2001), Double cusp: Model prediction and observational verification, *J. Geophys. Res.*, *106*, 25,571–25,593, doi:10.1029/2000JA000402.
- Wing, S., S. Ohtani, P. T. Newell, T. Higuchi, G. Ueno, and J. M. Weygand (2010), Dayside field-aligned current source regions, *J. Geophys. Res.*, *115*, A12215, doi:10.1029/2010JA015837.
- Zhao, H., C. P. Escoubet, R. Schmidt, Z. X. Liu, R. Grard, H. Laakso, K. Torkar, and F. Mozer (1999), Asymmetry of the position of the cusp observed by the Polar spacecraft, Proceedings of the Cluster II Workshop on Multiscale/Multipoint Plasma Measurements, Imperial College, London, ESA SP-449, p. 371.